Check for updates

Chemical Engineering & Technology

Chemical & Engineering Technology

RESEARCH ARTICLE

Co-Gasification of Lignite and Olive Kernel in Fluidized Bed Reactor: Synergetic Effect of Biomass

Hazal Öztan[1,2] | Duygu Uysal[1] | Özkan Murat Doğan[1] | Bekir Zühtü Uysal[1]

[1]Chemical Engineering Department, Gazi University, Ankara, Türkiye | [2]Graduate School of Natural and Applied Sciences, Main Campus, Gazi University, Ankara, Türkiye

Correspondence: Duygu Uysal (duysal@gazi.edu.tr)

Received: 5 February 2025 | **Revised:** 25 November 2025 | **Accepted:** 12 December 2025

Keywords: biomass | co-gasification | fluidized bed | hydrogen production | syngas

ABSTRACT

In this work, steam co-gasification of Tunçbilek lignite and olive kernel was investigated in a lab-scale fluidized bed gasifier to evaluate the effects of temperature on gasification mechanism and synergy between lignite and olive kernel. Experiments were carried out at temperatures ranging between 600°C and 900°C. Fuels were prepared with different mass fractions (0:100, 25:75, 50:50, 75:25, and 100:0 olive kernel/lignite). As a result of this study, as temperature increased, the H_2 concentration in syngas increased. The optimum gasification temperature was obtained as 800°C for both fuels and also for their co-gasification. In addition, potassium content in olive kernel enhanced the co-gasification as a natural catalyst.

1 | Introduction

The increasing global energy demand is primarily met by conventional sources such as coal, oil, and natural gas. However, this demand is so substantial that existing fossil fuel reserves are widely recognized as limited [1]. Fossil fuels also pose significant challenges due to the greenhouse gas emissions generated by conventional energy systems and their associated environmental impacts. The Net Zero Emissions by 2050 Scenario plays a critical role in reducing greenhouse gas emissions and the global use of fossil carbon sources [2, 3]. Although annual investments in fossil fuels showed a slight increase between 2020 and 2023, investments in clean energy have simultaneously continued to grow. According to the 2023 report of the International Energy Agency (IEA), annual investment in fossil fuels reached $1.1 trillion, whereas investment in clean energy rose to $1.8 trillion in 2022 [4]. These trends clearly indicate the necessity of developing alternative energy production technologies and expanding the use of clean energy sources.

Coal is primarily composed of carbon, is combustible, and exhibits sedimentary characteristics, making it an important fossil fuel today. Its main constituents include carbon, hydrogen, oxygen, nitrogen, sulfur, and various inorganic compounds. Compared with other fossil fuels, coal can exhibit a wide range of elemental compositions; it may contain 65%–95% carbon, 2%–6% hydrogen, and up to 30% oxygen, along with sulfur and nitrogen [5]. The composition of coal varies with its geological formation and age, and its carbon content increases with the length of time it has remained underground. A summary of coal rank categories and the associated ASTM criteria is presented in Table 1.

Coals with the lowest carbon content are subbituminous coal and lignite [6]. Xia et al. reported that China, Australia, Türkiye, India, and the northern United States collectively hold approximately half of all global coal deposits, consisting mainly of bituminous coal and lignite [7]. According to the 2023 report of the Turkish Coal Enterprise, Türkiye's bituminous coal and lignite reserves account for 30% (320.47 Mt) of global coal reserves [8]. Lignite

Abbreviations: IEA, International Energy Agency; IEA/OECD, Organisation for Economic Co-operation and Development; L, lignite; OK, olive kernel.

© 2026 Wiley-VCH GmbH

TABLE 1 | Summary of coal rank categories and associated ASTM criteria [6].

Rank	Volatile matter content (% wt, wet-ash-free)	Carbon content (% wt, wet-ash-free)	Calorific value (Btu/lb, mineral-free)	Moisture content (% wt)
Lignite	69–44	76–62	8300–6300	52–30
Subbituminous	52–40	80–71	11 500–8300	30–12
Bituminous—High volatile B	52–40	80–71	11 500–8300	30–12
Bituminous—High volatile C	50–29	86–76	13 000–10 500	15–2
Bituminous—High volatile A	49–31	88–78	14 000	5–1
Bituminous—Medium volatile	31–22	91–86	14 000	5–1
Bituminous—Low volatile	22–14	91–86	14 000	5–1
Anthracite	14–2	99–91	14 000	5–1

reserves in Türkiye constitute a primary fossil energy source and play a vital role in national energy production. Önen and Karaoğlan reported that the largest lignite reserve is located in the Afşin–Elbistan basin, whereas another significant deposit is the Tunçbilek lignite in Kütahya province [9]. Tunçbilek lignite (as-received coal) has an upper calorific value of 1750 kcal/kg and a lower calorific value of 1501 kcal/kg [10]. Although Tunçbilek lignite is classified as a low-rank coal, it remains an important fossil resource for energy utilization in Türkiye. Moreover, research efforts continue to focus on its combustion behavior, the influence of ash content on combustion units and construction materials, char–mineral interactions, and underground coal gasification applications [11–14].

Olive (*Olea europaea* L.) belongs to the Oleaceae family. Its native regions include the upper parts of Mesopotamia, South-East Asia, and the Southeastern Anatolia region. The spread of the olive plant occurred in two main directions: one route through Egypt to Tunisia and Morocco, and the other via Anatolia to the Aegean islands, Greece, Italy, and Spain. European Union countries like Italy, Spain, and France are responsible for producing around 70% of the world's olives. Türkiye, Tunisia, and Morocco are also significant producers. In Türkiye, which has a total agricultural area of 27 million hectares, 2.2% is dedicated to olive groves [15]. Olive kernel is a fuel with high organic content, energy value close to lignite, low ash content, and low sulfur dioxide emission and is obtained in solid form through olive oil production processes. A total of 15–22 kg of olive oil and 35–45 kg of olive kernel are obtained from 100 kg of olives. Approximately 70% of the olive harvest is used in olive oil production and approximately 500 000 t (1 250 000 × 0.4) of olive kernel are produced from this process. This given amount of olive kernel is on a wet basis. If the moisture content of the raw olive kernel is assumed to be approximately 50%, the amount of olive kernel on a dry basis is estimated to be 250 000 t per year [16]. Olive kernel is one of the most significant biomass types in Mediterranean regions and Türkiye. Ceylan and Kendirli suggested that olive kernel can be combusted as a fuel aside from other fuels and they reported the properties of olive kernel used as fuel with 4847 and 4480 kcal/kg upper heating value and lower heating value, respectively [17].

Thermochemical conversion techniques are based mainly on using carbon sources to produce alternative gas and liquid products. Thermochemical conversion techniques include pyrolysis, gasification, and combustion. Gasification process is defined as reasonable, efficient, economic, and reliable technique to convert carbonaceous sources [18]. Gasification mainly relies on coal gasification worldwide, but nowadays carbon-neutral resources like biomass, waste, and residues are among the leading alternative sources [19]. Likewise, biomass gasification with coal is a reliable way to convert low-carbon-content resources. Biomass gasification with coal is defined as co-gasification, and this concept presents energy-saving, low-carbon utilization, clean production, and an efficient fuel conversion process. It is mentioned that the above-reported gas and liquid products are obtained from thermochemical conversion techniques. Mainly, a gas product is obtained from the gasification process, which is called syngas (synthesis gas). Syngas is a gas mixture of hydrogen and carbon monoxide. Moreover, another important component in syngas is methane. Syngas is such an important gas product because it contains two combustible gases (methane and carbon monoxide) and a major energy carrier, hydrogen [20]. Therefore, it can be used both in engines and to produce various chemicals like methanol, dimethyl ether, and Fischer–Tropsch products [21]. Nowadays, researchers globally focus on utilizing local coals and agricultural biomass sources as fuel for gasification [22–24].

Co-gasification has an interesting gasification mechanism due to the relationship between biomass and coal. Biomass addition in the coal feed affects the gasification mechanism. This effect is called synergy, and it influences the reactivity of the process. Co-gasification synergy and reactivity offer extremely important and efficient ways to utilize carbon-neutral and low-carbon local coals. In addition, as the gasification of coal with biomass

15214125, 2026, 2, Downloaded from https://onlinelibrary.wiley.com/doi/10.1002/ceat.70163 by HAZAL OZTAN - Gazi University , Wiley Online Library on [03/02/2026]. See the Terms and Conditions (https://onlinelibrary.wiley.com/terms-and-conditions) on Wiley Online Library for rules of use; OA articles are governed by the applicable Creative Commons License

positively supports the formation of biochar that occurs during the process, the conversion of carbon contained in the fuel can reach much higher values. Studies by De Oliveira et al., Faizan et al., and Fu et al. reported that the favorable biomass effect on gasification is observed owing to the synergistic behavior of biomass and coal [25–27]. Besides, Wei et al. investigated the synergistic behavior of straw coke and petroleum coke in gasification. The results indicated that as the biomass fraction in the feed increased, the reactivity of the fuels also increased [28]. Similarly, biomass in the feed is also important for fuel reactivity, because biomass resources contain many alkali/alkaline earth metals and also have high volatile matter in their original structure. This means that the alkali metal content acts as a natural catalyst, and the volatile matter helps to open extra pores in the fuel, especially in the coal structure. Extra pores in the fuel structure enhance the production of char during gasification. Several studies reported that adding biomass in the feed enhances the pore structure of carbonaceous fuels [29–31]. Although previous studies have demonstrated that biomass addition influences the gasification mechanism through synergistic interactions—enhancing reactivity, promoting pore formation, and facilitating higher carbon conversion as reported by De Oliveira et al., Faizan et al., Fu et al., and Wei et al. [25–28]—there remains a notable lack of research focusing on a specific and industrially relevant feedstock combination. More specifically, limited data are available on the co-gasification of Turkish lignite with high-potassium biomass under steam, despite the fact that potassium-rich biomass is known to provide catalytic effects and significantly intensify char reactivity and pore development [29–31].

This study directly addresses the research gap arising from the limited data on the steam co-gasification of Turkish lignite with high-potassium biomass, despite the strong catalytic influence of alkali metals on gasification reactions. Tunçbilek lignite is an important local coal reserve for Tunçbilek city in Türkiye and, although classified as a low-rank coal, it possesses a remarkable carbon content that makes it a valuable fossil-based resource for thermochemical conversion. Likewise, biomass not only contributes additional carbon but also supports hydrogen formation in syngas due to its volatile matter and inherent catalytic components, meaning that appraising the carbon in biomass and its contribution to hydrogen release is essential for understanding its gasification behavior and its potential as an alternative energy source. Building upon these perspectives and the known synergistic interactions between coal and biomass, the present work aims to (i) investigate the steam co-gasification behavior of Tunçbilek lignite and potassium-rich olive kernel in a fluidized bed gasifier, (ii) evaluate the effect of biomass ratio and temperature on syngas composition—particularly hydrogen formation—and (iii) elucidate the catalytic role of potassium through K/Al and K/Si ratios. The novelty of this research lies in providing the first comprehensive experimental evaluation of the synergy between Tunçbilek lignite and olive kernel under steam, offering new insight into the utilization of regionally abundant low-carbon resources for hydrogen-rich syngas production.

2 | Materials and Methods

In this experimental study, steam gasification of Tunçbilek lignite and olive kernel was studied to produce syngas in a laboratory-scale fluidized bed reactor. Lignite and olive kernel were used as fuels in the reactor. Tunçbilek lignite was supplied from Kütahya by the Turkish Coal Enterprise. Likewise, olive kernel was obtained from olive oil producers in Çanakkale province. Lignite and olive kernel samples were prepared by crushing and performing sieve analysis for the experimental studies. Physical properties such as average particle diameter and bulk density of the fuels were determined. The average particle diameters of the fuels were 0.4 mm for lignite and 1.1 mm for olive kernel. Bulk densities for lignite and olive kernel were measured as 1341 and 1146 kg/m^3, respectively. In addition, fuels were analyzed to obtain percentages of moisture, ash, volatile matter, and fixed carbon contents via the proximate analysis method. All proximate and ultimate analyses were performed on an as-received basis. Proximate analysis of fuels was carried out according to the standards, which are ASTM D3173 for moisture content, TS 711 ISO 562:2014 for volatile matter content, TS ISO 1171 for ash content, and fixed carbon content was determined by difference. The details about the proximate analysis method can be found in another gasification study of the authors [32]. The proximate analysis results of the fuels were presented in Table 2. Ultimate analysis of the fuels was done using a Leco CHN 1000 device. Ultimate analysis results are presented in Table 3. Furthermore, fuels were analyzed by the R&D Laboratory of Meta Nickel Cobalt Mining Industry and Trade Plc. in order to detect their metal contents. The metal contents of the fuels were determined using an Agilent A-G8462AA ICP-OES device. The metal content results are given in Table 4.

TABLE 2 | Proximate analysis of Tunçbilek lignite and olive kernel (as-received basis).

Content (%)	Tunçbilek lignite	Olive kernel
Moisture	13.51	5.86
Ash	13.72	3.16
Volatile matter	34.39	65.12
Fixed carbon	38.38	25.86

TABLE 3 | Ultimate analysis of Tunçbilek lignite and olive kernel (as-received basis).

Content (%)	Tunçbilek lignite	Olive kernel
C	56.89	50.5
H	4.28	6.55
O	7.97	32.33
N	2.16	1.39
S	1.47	0.21
Moisture	13.51	5.86
Ash	13.72	3.16

Gasification experiments were carried out in a laboratory-scale fluidized bed reactor. The designed reactor was operated according to the average particle diameters and densities of the fuels, and the minimum fluidization velocity of steam in the reactor was calculated as 0.042 m/s, and the superficial velocity was set

15214125, 2026, 2, Downloaded from https://onlinelibrary.wiley.com/doi/10.1002/ceat.70163 by HAZAL OZTAN - Gazi University , Wiley Online Library on [03/02/2026]. See the Terms and Conditions (https://onlinelibrary.wiley.com/terms-and-conditions) on Wiley Online Library for rules of use; OA articles are governed by the applicable Creative Commons License

TABLE 4 | Metal contents of Tunçbilek lignite and olive kernel.

[mg/kg dry fuel]	Al	Ca	Fe	Mg	Na	Ni	K	Si	Zn
Tunçbilek lignite	23.26	2.50	14.06	5.44	0.55	0.61	4.36	47.93	0.04
Olive kernel	1.22	12.98	6.18	2.63	4.69	0.19	35.24	35.44	0.05
[mg/kg dry fuel]	**Ag**	**As**	**Cd**	**Co**	**Cr**	**Cu**	**Mn**	**Pb**	**Sc361**
Tunçbilek lignite	0.005	23.66	0.005	0.008	0.34	0.03	0.22	0.005	0.006
Olive kernel	0.01	0.51	0.01	0.01	0.11	0.03	0.60	0.01	0.01

as $U = 3U_{mf}$. The residence time (τ) was estimated using $\tau = V/Q$, where V is the effective reactor volume above the distributor and Q is the volumetric steam flow rate at the reaction temperature. For the fixed steam flow rate of 7 g/min under atmospheric pressure, the gas residence time was approximately 49 s at 600°C and decreased to about 36 s at 900°C, that is, falling within the range of 36–50 s for all experimental conditions. In addition, flow rate of steam was set as three times the minimum fluidization velocity in the reactor. Hence, the flow rate of steam was supplied to the reactor as 7 g/min. This value is also the optimum value for the Tunçbilek lignite and olive kernel gasifications owing to steam/fuel ratio, and the optimization work was clearly presented in Öztan et al. [33]. When the steam/fuel ratio was considered 0.7 g steam/g fuel, 10 g of fuels which are different mixtures by weight of Tunçbilek lignite and olive kernel were prepared and fed to the gasifier. The fuel mixtures were prepared with mass ratios of olive kernel and Tunçbilek lignite as 25:75, 50:50, 75:25, 100:0 OK: lignite, and 0:100. Experiments were carried out at four different temperatures which are 600°C, 700°C, 800°C, and 900°C and the reactor was operated at atmospheric condition. Schematic diagram of the gasification system is presented in Figure 1. The reactor was made up of quartz glass. The height of the reactor was measured as 1.3 m. It has 0.05 m inner diameter (D1) at the bottom, and that of the freeboard (D2) is 0.2 m. It was externally heated by a vertical electrical furnace, and an indirect heating gasification approach was carried out. A perforated plate which was made of stainless steel was used as a distributor. The distributor was located 0.25 m above from the bottom of the reactor and had 38 holes that were 0.0015 m in diameter. Silica sand, 310 μm in diameter, was used as the bed material. Steam, as gasification agent, was produced with a steam generator at 100°C and was fed from the bottom of the reactor. The fluidized bed reactor was equipped with a cyclone, a temperature controller, and a thermocouple. Dehumidification bottles with silica gel were used to prevent moisture from reaching the gas chromatography device and to clean the produced syngas. Besides, hot outlet stream of syngas was cooled via condensers. The fuel was fed using a screw feeder from the top of the reactor. Moreover, the whole system was isolated with fiberglass. The produced syngas was collected in gas sampling bags and was analyzed with SRI 310 model TCD gas chromatography device to examine hydrogen, carbon monoxide, carbon dioxide, and methane contents. The gas chromatograph was equipped with a silica gel column of 3′ × 1/8″ (length × diameter). Argon was used as the carrier gas. Syngas samples were injected into the column using a 1 μL Hamilton microsyringe. The injection was completed within approximately 1–2 s, which is typical for manual gas injection and does not influence chromatographic separation or peak resolution under the operating conditions of our GC system. The chromatographic signals were recorded and processed using the PeakSimple software package. The temperature program of the gas chromatograph is provided in Table 5. All gasification experiments were performed in triplicate ($n = 3$), and the reported values represent the average of the repeated runs. Gas compositions were measured using a GC analyzer with an accuracy of ±0.5%, temperatures were recorded with a thermocouple of ±1°C sensitivity, and mass measurements were obtained with a balance precision of ±0.001 g.

3 | Results and Discussion

In this study, Kütahya-Tunçbilek lignite and olive kernel were gasified with steam to obtain hydrogen-rich syngas. Therefore, a lab-scale fluidized bed reactor was designed and experimental studies were carried out at 600°C, 700°C, 800°C, and 900°C. Tunçbilek lignite and olive kernel were gasified separately in the first step and temperature effects on the gasification mechanism were investigated. In addition, effect of olive kernel in the fuel mixture was examined experimentally, and hydrogen concentration in the produced syngas was discussed. Besides, natural catalytic effects of the alkali metal content of the fuels were clarified using the K/Al and K/Si ratio of fuel mixtures.

Gasification reactions are equilibrium reactions, and they occur simultaneously in the reactor. Gasification reaction mechanism is defined by mainly five reactions, namely, water–gas, water–gas shift, Boudouard, methanation, and steam methane reforming reactions. Water–gas reaction (1) is the major reaction of carbonaceous materials for producing syngas. Besides, water–gas shift reaction (2) is the most important point of the steam gasification to increase the hydrogen concentration in syngas. This reaction occurs kinetically in high gasification temperatures in the presence of excess steam and, it is thermodynamically limited at low temperatures [34–36]. The Boudouard (3) and methanation (4) reactions are also important gasification reactions. The Boudouard and water–gas reactions are favored at high gasification temperatures and low pressures. However, the methanation reaction requires low temperatures and high pressures. The steam methane reforming reaction (5) takes place at high gasification temperatures [37].

Water gas reaction

$$C_{(s)} + H_2O_{(g)} \leftrightarrow CO_{(g)} + H_{2(g)} \quad \Delta H^\circ = +131.38 kJ/mol \quad (1)$$

15214125, 2026, 2, Downloaded from https://onlinelibrary.wiley.com/doi/10.1002/ceat.70163 by HAZAL OZTAN - Gazi University , Wiley Online Library on [03/02/2026]. See the Terms and Conditions (https://onlinelibrary.wiley.com/terms-and-conditions) on Wiley Online Library for rules of use; OA articles are governed by the applicable Creative Commons License

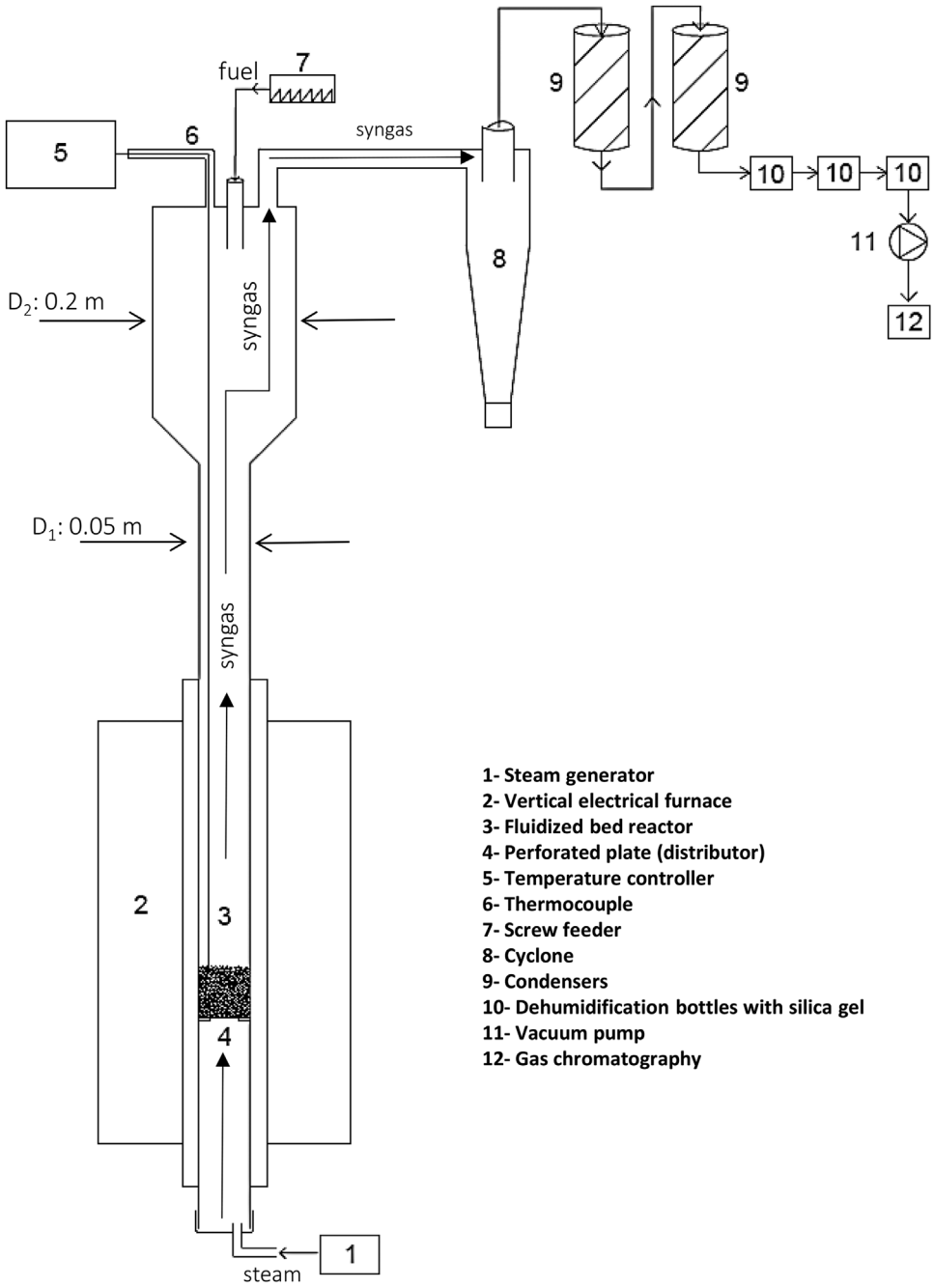


FIGURE 1 | Schematic diagram of the gasification system.

Water gas shift reaction

$$CO_{(g)} + H_2O_{(g)} \leftrightarrow CO_{2(g)} + H_{2(g)} \quad \Delta H^\circ = -41.15 kJ/mol \quad (2)$$

Boudouard reaction

$$C_{(s)} + CO_{2(g)} \leftrightarrow 2CO_{(g)} \quad \Delta H^\circ = +172.58 \ kJ/mol \quad (3)$$

Methanation reaction

$$C_{(s)} + 2H_{2(g)} \leftrightarrow CH_{4(g)} \quad \Delta H^\circ = -74.90 \ kJ/mol \quad (4)$$

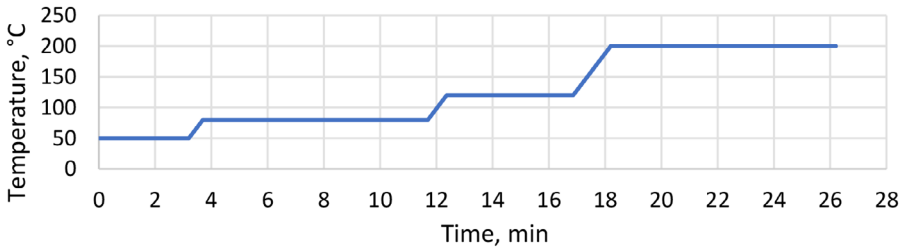
Steam methane reforming reaction

$$CH_{4(g)} + H_2O_{(g)} \leftrightarrow 3H_{2(g)} + CO_{(g)} \quad \Delta H^\circ = +206 \ kJ/mol \quad (5)$$

Temperature is one of the important parameters for gasification reactions as stated above, as it affects the gas composition of syngas and carbon conversion due to the equilibrium among the gasification reactions and their kinetics [38]. Numerous studies have highlighted the effects of temperature on coal and biomass gasification. Regarding these, suitable temperature interval for coal gasification is reported as 750–1000°C [39], and 550–900°C for biomass gasification [40]. Ash and volatile matter content of fuels, NO_x emissions, and material of construction of the reactor affect the gasification temperature limits. Regarding these

15214125, 2026, 2, Downloaded from https://onlinelibrary.wiley.com/doi/10.1002/ceat.70163 by HAZAL OZTAN - Gazi University , Wiley Online Library on [03/02/2026]. See the Terms and Conditions (https://onlinelibrary.wiley.com/terms-and-conditions) on Wiley Online Library for rules of use; OA articles are governed by the applicable Creative Commons License

TABLE 5 | GC temperature programming parameters.

Initial temperature (°C)	Hold time (min)	Heating rate (°C/min)	Final temperature (°C)
50.00	3.200	60.00	80.00
80.00	8.000	60.00	120.00
120.00	4.500	60.00	200.00
200.00	8.000	0.00	0.00
Graphical representation			

limitations, in this study, it was aimed to prevent ash fusion inside gasifier owing to the high ash content of Tunçbilek lignite, as high ash content, resulting in ash fusion, can cause blockage in the bed and disturb the fluidization regime. The ash contents presented in Table 2 were taken into consideration when selecting the operating temperature range for the fluidized bed gasification experiments. The experiments were conducted between 600°C and 900°C in order to remain safely below the expected ash softening and fusion temperatures associated with the mineral composition of the fuels. Operating within this controlled temperature window minimizes the risk of ash melting, agglomeration, or bed defluidization inside the reactor. Preventing such phenomena is one of the primary technical objectives of the system, and the selected temperature range ensures stable gasification behavior and reliable experimental performance. In addition, volatile matter helps with the pyrolysis and char formation before gasification [41]. The olive kernel has higher volatile content than the lignite (Table 2). Therefore, it is aimed to prevent excessive volatilization of the matter in biomass. Regarding all these, the gasification temperature interval was selected as 600–900°C for this study. In the experiments, first, Tunçbilek lignite and the olive kernel were gasified separately in the presence of steam in the fluidized bed. In this part of the study, optimum gasification temperatures for the fuels were obtained experimentally to produce hydrogen-rich syngas (Table 6). Experimental results of syngas contents produced from Tunçbilek lignite and olive kernel steam gasifications are presented in Figures 2 and 3.

As can be seen from the results, increasing gasification temperature enhanced the hydrogen concentration in produced syngas for both fuels. The temperature interval enhancing the hydrogen concentration was found to be 600–800°C. Within this interval, the water–gas reaction is favored to produce hydrogen and carbon monoxide gases. Moreover, the two carbon consuming reactions which are water–gas and Boudouard reactions are at equilibrium within this temperature interval. The presented study shows that the equilibrium constant of the water–gas reaction is greater than that of the Boudouard [28], which indicates that the carbon content of fuels is more significantly consumed by water–gas reaction to produce hydrogen than Boudouard reaction. Likewise, water–gas-shift reaction influences the hydrogen release in syngas when the feed stream has high steam content [42]. The highest hydrogen concentrations for lignite and olive kernel gasification were obtained at 800°C as 92.9% and at 900°C 94.3%, respectively. This result is in good agreement with the literature studies. Vêlez et al. investigated the effect of temperature in coal gasification and reported that as the gasification temperature was increased, the concentration of hydrogen in syngas increased, and also optimum gasification temperature is reported to be 820°C [43]. Similarly, Almeida et al. and Hofbauer and Rauch noted that increment in temperature affects the syngas composition positively in biomass and waste gasification, and hydrogen concentration increases as the temperature is increased. Optimum gasification temperatures in these studies are reported as 885°C and 800°C, respectively [44, 45]. Furthermore, other presented studies about gasification temperature effects for lignite and olive kernel are in good agreement with enhancing of temperature [46–49]. It should be noted that in the gasification process of olive kernel, the temperature must be increased by approximately 100°C for a 1.7% increase in hydrogen concentration. As there is no significant concentration increase, the use of 800°C instead of 900°C is recommended in this study as the optimum condition.

Besides, the fixed carbon content of the fuels is the second important point for gasification. It is clearly seen from the experimental results that the hydrogen concentrations obtained from Tunçbilek lignite gasification are greater than those of olive kernel gasification because of the higher fixed carbon content of the lignite (Table 2), as fixed carbon content enhances steam–char gasification and char reactivity to produce hydrogen. When temperatures higher than 800°C were applied, the water–gas reaction did not dominate the gasification, and thus the hydrogen release decreased. In addition, the Boudouard reaction dominated the reaction mechanism instead of the water–gas reaction, and carbon monoxide was produced by consuming char and carbon dioxide. This is because the relationship between carbon monoxide and carbon dioxide gases is quite complicated, as equilibrium affects the syngas composition in the gasifier in relation to temperature.

15214125, 2026, 2, Downloaded from https://onlinelibrary.wiley.com/doi/10.1002/ceat.70163 by HAZAL OZTAN - Gazi University , Wiley Online Library on [03/02/2026]. See the Terms and Conditions (https://onlinelibrary.wiley.com/terms-and-conditions) on Wiley Online Library for rules of use; OA articles are governed by the applicable Creative Commons License

TABLE 6 | Summary of syngas composition (H_2, CO, CO_2, CH_4 vol%) for all biomass–lignite blends at different temperatures.

Fuel	*T* (°C)	H_2 (V/V%)	CH_4 (V/V%)	CO (V/V%)	CO_2 (V/V%)
0:100 OK:L	600	83.19	0	3.32	13.49
0:100 OK:L	700	86.94	0	0.6	12.46
0:100 OK:L	800	98.97	0	1.03	0
0:100 OK:L	900	94.06	0	0.59	5.35
100:0 OK:L	600	40.67	38.22	21.11	0
100:0 OK:L	700	64.76	12.68	13.41	9.15
100:0 OK:L	800	97.55	0.88	1.57	0
100:0 OK:L	900	95.33	1.16	3.51	0
25:75 OK:L	600	79.42	0	9.88	10.7
25:75 OK:L	700	81.05	0	0	18.95
25:75 OK:L	800	95.05	0	0	4.95
25:75 OK:L	900	95.65	0	0	4.35
50:50 OK:L	600	70.9	0	0	29.1
50:50 OK:L	700	79.53	0	0	20.47
50:50 OK:L	800	97.09	0	0	2.91
50:50 OK:L	900	96.99	0.36	0	2.65
75:25 OK:L	600	69.33	0	3.07	27.6
75:25 OK:L	700	76.46	0	0	23.54
75:25 OK:L	800	97.31	0.08	2.2	0.41
75:25 OK:L	900	94.67	0	0	5.33

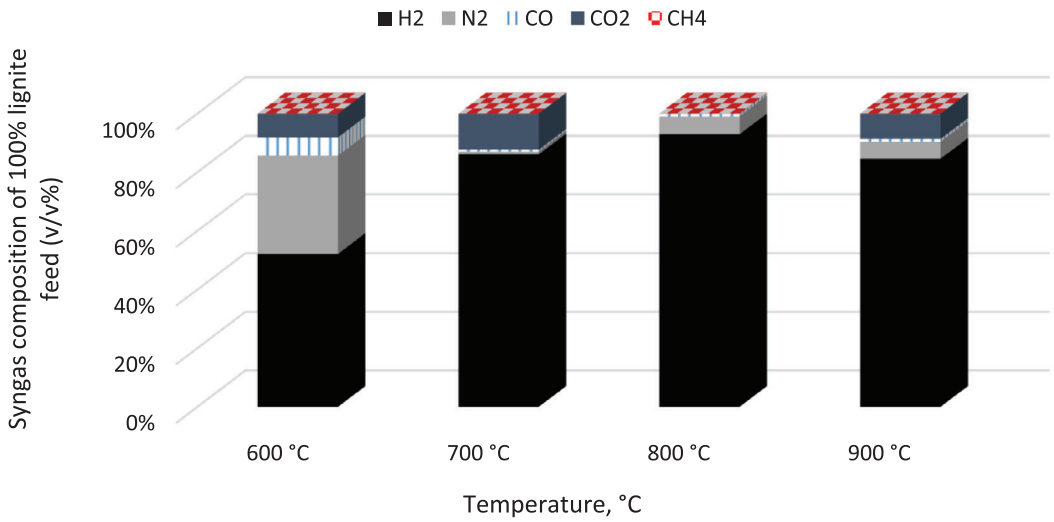


FIGURE 2 | Syngas composition of 100 (w/w%) Tunçbilek lignite feed.

Furthermore, due to the high oxygen content in the raw material may lead to combustion reactions (Equations 6–7) and to the releasing different compounds like hydrocarbons, chlorine, and tar, and therefore it is an important parameter in gasification systems. Due to the fact that syngas has combustible gases like carbon monoxide, methane, and volatiles, combustion reactions may take place during the gasification [50]. Due to its lower fixed carbon content and higher volatile matter content, olive kernel displayed gasification behavior rather than combustion behavior. Consequently, it can be stated that the likelihood of combustion reactions occurring in the gasifier is higher during lignite experiments, as evidenced by the carbon dioxide concentrations. As seen from Table 3, oxygen content of the olive kernel is higher than that of the lignite. Accordingly, carbon monoxide concentrations of the syngas produced from olive kernel were greater than those from lignite gasification results. It should not

15214125, 2026, 2, Downloaded from https://onlinelibrary.wiley.com/doi/10.1002/ceat.70163 by HAZAL OZTAN - Gazi University , Wiley Online Library on [03/02/2026]. See the Terms and Conditions (https://onlinelibrary.wiley.com/terms-and-conditions) on Wiley Online Library for rules of use; OA articles are governed by the applicable Creative Commons License

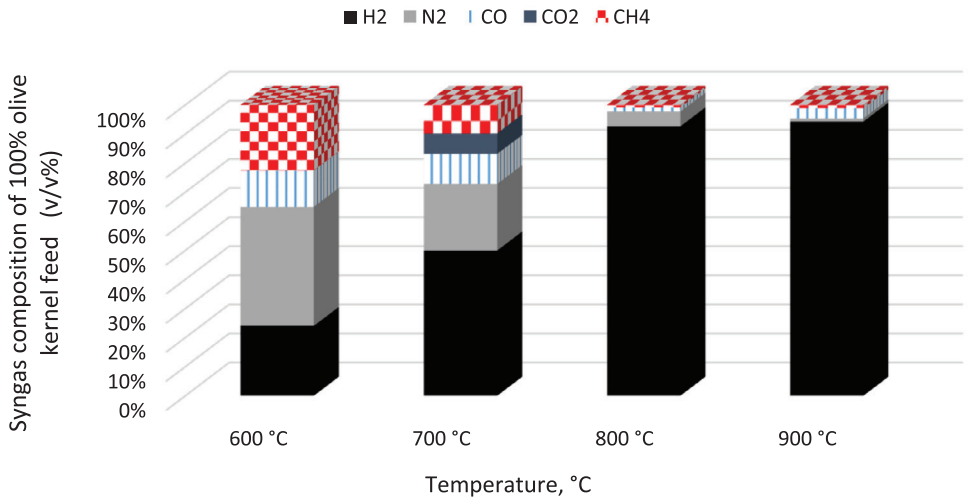


FIGURE 3 | Syngas composition of 100 (w/w%) olive kernel feed.

be forgotten that the conversion of carbon monoxide into carbon dioxide through the water–gas shift reaction, which increases hydrogen concentration and consumes carbon monoxide, was more pronounced in 100% lignite gasification. In contrast, carbon monoxide concentrations were higher in the 100% olive kernel gasification experiments compared to those with lignite.

Complete oxidation

$$C_{(s)} + O_{2(g)} \rightarrow CO_{2(g)} \quad \Delta H^{\circ} = -393.5 \ \text{kJ/mol} \qquad (6)$$

Partial oxidation

$$C_{(s)} + \frac{1}{2} O_{2(g)}\% \rightarrow CO_{(g)} \quad \Delta H^{\circ} = -110.5\% \ \text{kJ/mol} \qquad (7)$$

Syngas can also be a raw material to produce methane gas aside from hydrogen. Methane can be released during gasification when the volatile matter content of the fuel is high. Moreover, when the elemental hydrogen content of the fuel is high, methane production by means of the methanation reaction in gasification becomes significant at low temperatures. Because the olive kernel's volatile matter content is greater than that of lignite, methane gas was obtained from olive kernel gasification at 600°C and 700°C, whereas the syngas produced from lignite did not contain any methane gas (Figures 2 and 3). In addition, as the high amount of volatile matter in the olive kernel supports methane release regardless of the gasification temperature, even trace amounts of methane gas were observed in the syngas concentrations obtained in this experimental study. It is noted that the most suitable temperature was specified as 600°C to obtain maximum concentration of methane from olive kernel. Apart from these, produced methane in syngas was consumed by steam methane reforming reaction (Equation 5) with increasing temperature and promoted the hydrogen release which is in good agreement with the statements in literature [51–53].

The co-gasification concept is based on the gasification of coals and various biomasses together. In the process, the production of hydrogen-rich syngas is aimed, and the goal is also to increase the gas efficiency with higher methane concentration. Co-gasification synergy is the first important point regarding syngas content and carbon conversion as all kinds of coals and biomasses do not show the same behavior in co-gasification. Some types of biomass sources may increase the hydrogen concentration in the produced syngas, but some of them may decrease it or they can increase the methane and hydrocarbon concentrations in co-gasification. The second important point in co-gasification is the amount of biomass in the fuel as the amount of biomass affects the syngas composition and gas efficiency. Therefore, co-gasification synergy and the amount of biomass in the fuel are the main topics for obtaining hydrogen-rich syngas when considering the production of chemicals from syngas. In the co-gasification experiments of Tunçbilek lignite and olive kernel, the effect of olive kernel in the fuel on syngas composition was investigated experimentally. Experiments were carried out in the same gasification system. Ten grams of fuel were prepared in the weight ratio of olive kernel:lignite (OK:L) as 25:75, 50:50, and 75:25. Temperature was changed in the range of 600–900°C. The obtained syngas was analyzed with gas chromatography. Syngas compositions of the co-gasification experiments were presented for the fuels in Figures 4–6. Moreover, Table 6 presents the composition of the obtained syngas.

In the co-gasification experiments, hydrogen concentration increased with increasing gasification temperature in the range of 600–800°C. The highest hydrogen concentrations in syngas were obtained at 800°C for the 50:50 and 75:25 OK:L feeds as 76.7% and 49.4%, respectively. Additionally, the maximum hydrogen concentration for the 25:75 OK:L feed was obtained as 80.2% at 900°C. The effect of olive kernel on hydrogen concentration was investigated based on the fuel fed to the gasifier. It was determined that hydrogen concentration in the produced syngas decreased when olive kernel was added to the Tunçbilek lignite feed at ratios of 25%, 50%, and 75% (under constant temperature conditions). When Figure 7 is examined, hydrogen concentrations at gasification temperatures of 800°C and 900°C decreased compared to those obtained from 100% Tunçbilek lignite and 100% olive kernel feeds. If 800°C and 900°C are considered the regions where maximum hydrogen concentration can be obtained, adding olive kernel to the feed negatively affects the gasification behavior. In the literature similar effects were reported for hydrogen concentration in co-gasification studies in fluidized beds [54, 55]. Emami

15214125, 2026, 2, Downloaded from https://onlinelibrary.wiley.com/doi/10.1002/ceat.70163 by HAZAL OZTAN - Gazi University , Wiley Online Library on [03/02/2026]. See the Terms and Conditions (https://onlinelibrary.wiley.com/terms-and-conditions) on Wiley Online Library for rules of use; OA articles are governed by the applicable Creative Commons License

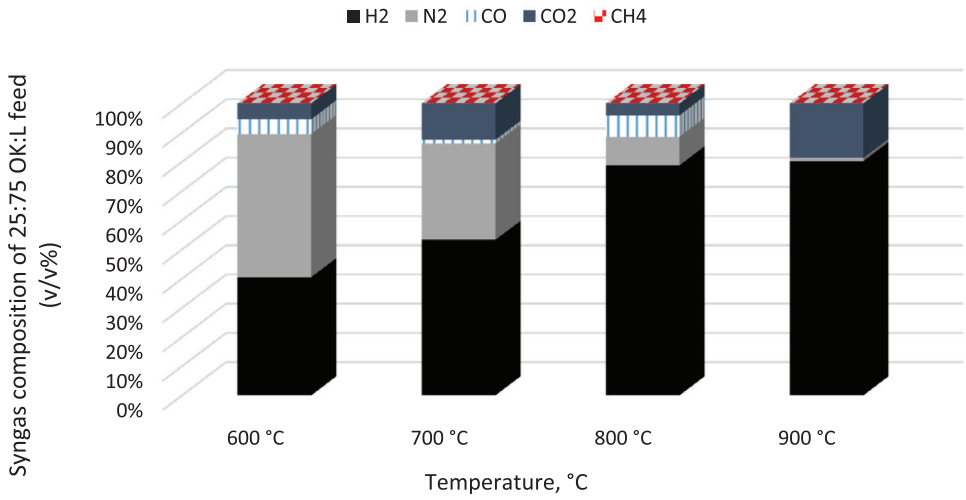


FIGURE 4 | Syngas composition of 25:75 (w/w%) OK:L feed.

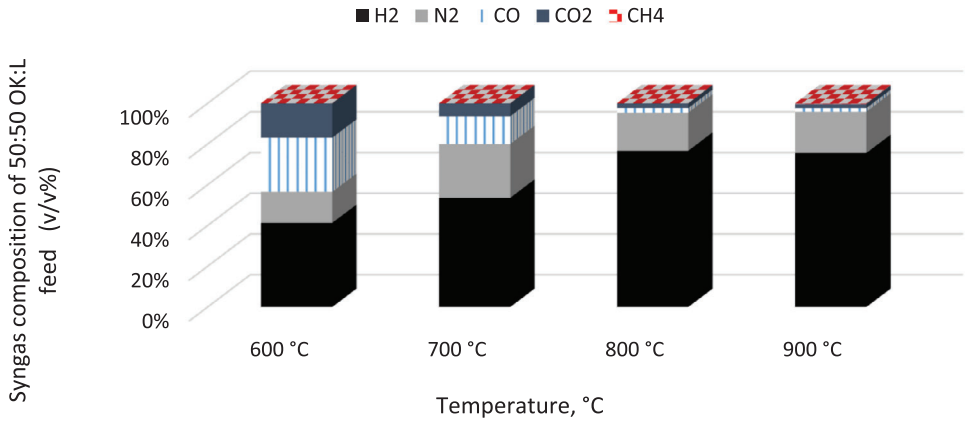


FIGURE 5 | Syngas composition of 50:50 (w/w%) OK:L feed.

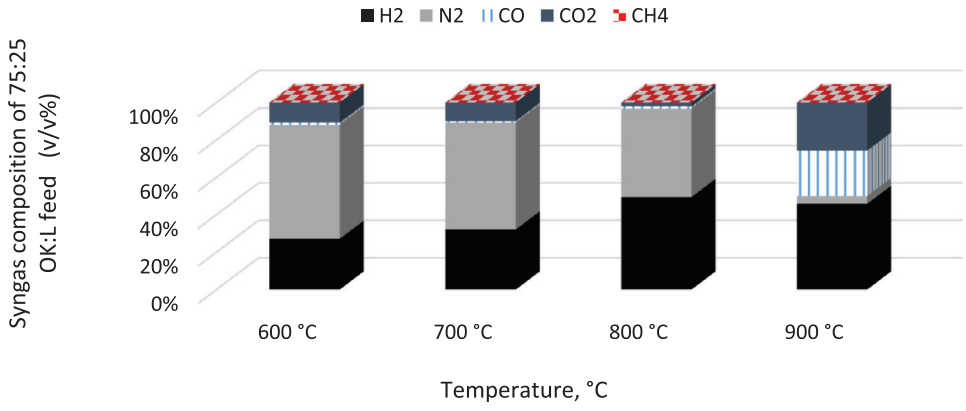


FIGURE 6 | Syngas composition of 75:25 (w/w%) OK:L feed.

Taba et al. reported that with the increasing amount of olive kernel in the fuel hydrogen percentages decreased because of the high volatile matter content in olive kernel [38]. This is because high volatile matter content may reduce the local temperature of the gasification region thus affecting carbon conversion and hydrogen release.

One of the most important points in co-gasification is the presence of alkali metals in biomass sources and also the Al–Si content of coals as they exhibit natural catalytic effects on co-gasification. There are three types of inorganic material that show natural catalytic effects in gasification: alkali metals, alkaline earth metals, and transition metals. Aside from the alkaline earth

15214125, 2026, 2, Downloaded from https://onlinelibrary.wiley.com/doi/10.1002/ceat.70163 by HAZAL OZTAN - Gazi University , Wiley Online Library on [03/02/2026]. See the Terms and Conditions (https://onlinelibrary.wiley.com/terms-and-conditions) on Wiley Online Library for rules of use; OA articles are governed by the applicable Creative Commons License

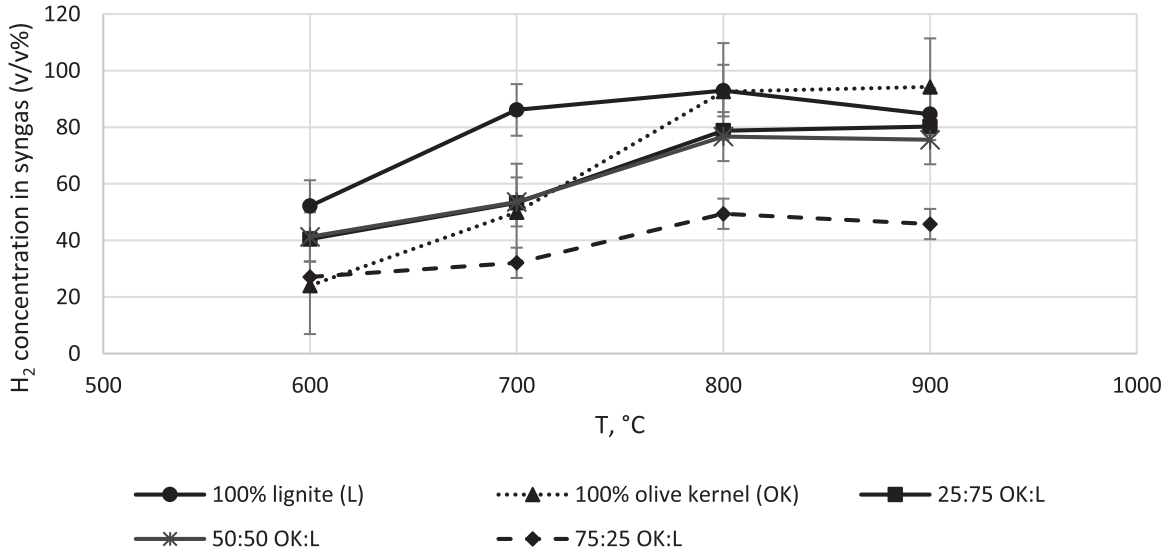


FIGURE 7 | Effect of amount of olive kernel in fuel on hydrogen concentration (fuel: w/w%).

and transition metals, the carbonated forms of alkali metals—especially K, Na, Ca, Li, and Mg—are used as catalysts in coal and biomass gasification. Among these—K, Na, and Li—show a higher positive catalytic effect compared to Ca and Mg. The results obtained in this study are in good agreement with the literature [56, 57]. When examining the effects of the feed ratios, the olive kernel-lignite mixtures prepared at ratios of 25:75, 50:50, and 75:25 showed a natural catalytic effect during the gasification process at 600°C, positively influencing the hydrogen concentration in the syngas. When Figure 7 is examined, it can be seen that the hydrogen concentrations for all three feed ratios are higher than those of 100% olive kernel feed at 600°C.

Apart from the temperature effects, the K/Al and K/Si ratios play an important role in their natural catalytic effects on gasification. If the fuel has K/Al ratio of about 1, the natural catalytic effect acts positively, and more hydrogen gas can be released [58]. On the other hand, the Al and Si contents in coal ash affect the gasification negatively because of the formation of aluminosilicates such as $KAlSiO_4$, $KAlSi_3O_8$, and $CaAl_2Si_2O_8$ [50, 59]. In the experiments, the prepared fuels of 25:75, 50:50, and 75:25 (OK:L) content had K/Al and K/Si ratios, respectively, as K/Al:0.34–K/Si:0.16 (25:75 feed ratio), K/Al:0.65–K/Si:0.26 (50:50 feed ratio), and K/Al:1.17–K/Si:0.36 (75:25 feed ratio).

When considering the results of the 25:75 and 50:50 feed ratios at a gasification temperature of 700°C, it is clearly seen that the hydrogen concentration is again supported by the natural catalytic effect. Even though the fixed carbon content decreases with the addition of olive kernel in the 50:50 feed ratio, the positive influence of the 0.65 K/Al and 0.26 K/Si ratios allowed the hydrogen concentration to be very close to that of the 25:75 feed ratio. Although it has the lowest fixed carbon content compared with the others, the fuel at the ratio of 75:25 (OK:L) supported the hydrogen release in syngas owing to its high K/Al ratio. The mixture at the 25:75 (OK:L) ratio has the lowest K/Al ratio, yet it has a high fixed carbon content, and its K/Si ratio is the lowest among the mixtures. Therefore, it can be said that the lowest K/Si ratio prevented the formation of aluminosilicates. The results of the fuel at the ratio of 50:50 (OK:L) are between the results of the 25:75 and 75:25 (OK:L) fuels. The obtained results are in good agreement with literature [60–65].

To investigate the mechanistic influence of mineral composition on hydrogen formation, the K/Al ratios derived from the ash analyses of the blended fuels were correlated with the hydrogen amount measured at 800°C. The comparison presented in Figure 8 demonstrates a clear positive association between the K/Al ratio and hydrogen production. This trend indicates that potassium-rich mineral phases play an active catalytic role in gasification chemistry, particularly by promoting secondary devolatilization, accelerating tar cracking, and enhancing steam–char reforming reactions. Potassium species are known to increase the concentration of surface oxygenated functional groups and to lower the activation barriers for C–O–H reaction pathways, leading to higher rates of hydrogen-forming reactions at elevated temperatures. In contrast, alumina-rich structures tend to be less catalytically active, and therefore blends with lower K/Al ratios exhibit comparatively reduced hydrogen amounts. Although the dataset is limited by the number of available ash analyses, the consistent monotonic increase in hydrogen amount with increasing K/Al ratio supports the conclusion that the relative abundance of potassium to aluminosilicate phases is a key determinant of catalytic activity in high-temperature gasification environments. This observation aligns well with established mechanisms of alkali-induced enhancement of char reactivity and confirms that mineralogical differences among the blends contribute measurably to the observed variation in hydrogen formation.

Hydrogen formation did not increase monotonically with higher potassium contents because high olive kernel proportions introduce an additional thermal effect. Olive kernel contains a large amount of volatile matter, and its rapid release at elevated blending ratios leads to localized cooling within the gasification zone. This temperature drop suppresses high-temperature reaction pathways such as steam–char reforming and tar reforming, which are major contributors to hydrogen production. Therefore,

15214125, 2026, 2, Downloaded from https://onlinelibrary.wiley.com/doi/10.1002/ceat.70163 by HAZAL OZTAN - Gazi University , Wiley Online Library on [03/02/2026]. See the Terms and Conditions (https://onlinelibrary.wiley.com/terms-and-conditions) on Wiley Online Library for rules of use; OA articles are governed by the applicable Creative Commons License

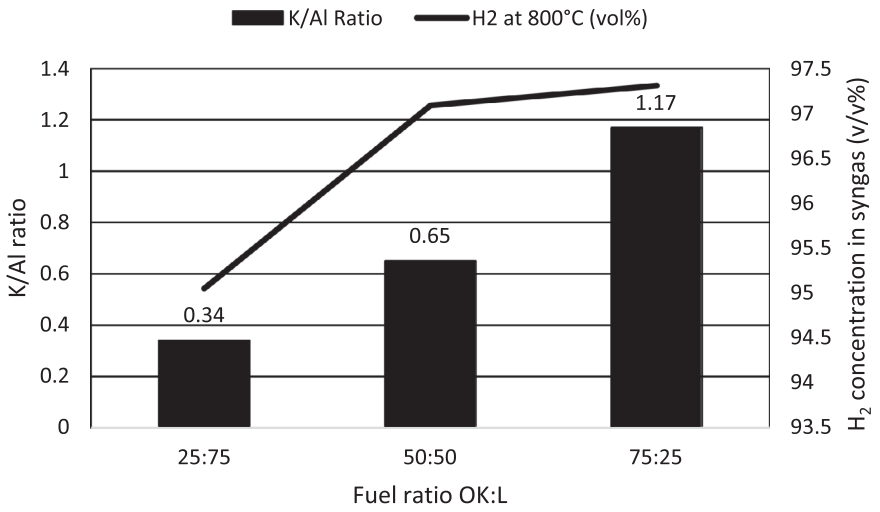


FIGURE 8 | Effect of K/Al ratio on H_2 formation at 800°C.

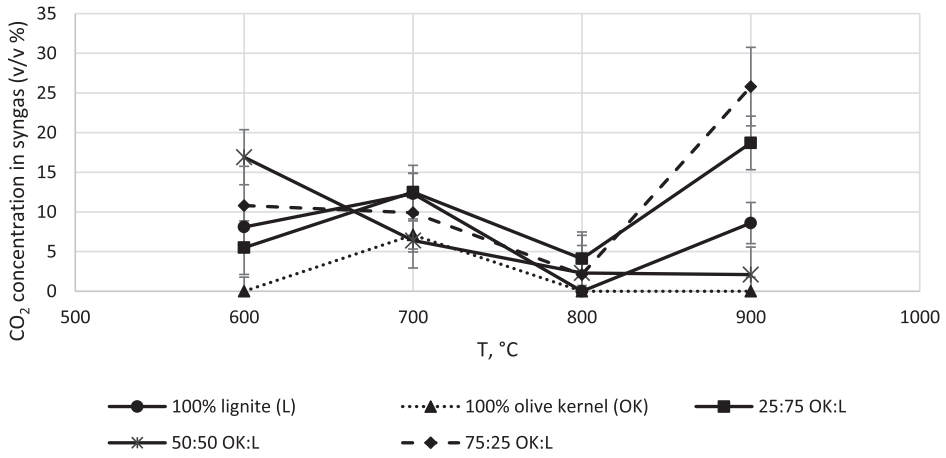


FIGURE 9 | Effect of amount of olive kernel in fuel on carbon dioxide concentration (fuel: w/w%).

even though the ash of OK-rich blends contains higher K concentrations that would theoretically favor catalytic enhancement, the effective reaction temperature is reduced, resulting in a lower hydrogen amount. This interplay between mineral catalysis and volatile-induced temperature reduction explains the observed deviation from a strictly potassium-driven trend (Figure 7).

In order to highlight the key quantitative outcomes of the study, the maximum hydrogen amounts obtained for each fuel and blend were summarized. Pure lignite amount its highest hydrogen amount at 800°C with 98.97 vol%, whereas pure olive kernel reached 97.55 vol% at the same temperature. Among the blends, the 25% olive kernel–75% lignite mixture achieved 95.65 vol% H_2 at 900°C, whereas the 50% olive kernel–50% lignite blend produced 97.09 vol% H_2 at 800°C. The highest value among the biomass-rich mixtures was observed for the 75% olive kernel–25% lignite blend, which reached 97.31 vol% at 800°C. These results collectively demonstrate that both the blending ratio and operating temperature strongly influence hydrogen formation during gasification.

In Figures 9 and 10, a significant decrease in carbon monoxide concentrations in the co-gasification is observed between 600°C and 800°C. This decrease in concentrations occurred as a result of the consumption of carbon monoxide through the water–gas shift reaction, which supports hydrogen production. Another result that supports this situation is the increase in carbon dioxide concentrations. Although an increase is observed between 600°C and 700°C, it can be easily interpreted that, with the increase in temperature between 700°C and 800°C the equilibrium of the Boudouard reaction shifts to the right consuming carbon dioxide as a reactant. The complex relationship between carbon monoxide and carbon dioxide gases due to the water–gas shift and Boudouard reactions results in instantaneous reaction equilibria in the gasifier, consuming reactants or products and preventing extreme increases or decreases in carbon monoxide and carbon dioxide concentrations. Moreover, methane release in co-gasification was not observed during the experiments. The main reason for the absence of methane in the syngas produced during co-gasification is the high gasification temperatures. As is known, the methanation reaction is not supported at high temperatures. In addition to the high temperature, another important parameter is the use of steam as a gasification agent. The use of steam causes any methane that could be released due to the nature of the olive kernel (high volatile matter content) during gasification to be consumed through the steam–methane

15214125, 2026, 2, Downloaded from https://onlinelibrary.wiley.com/doi/10.1002/ceat.70163 by HAZAL OZTAN - Gazi University , Wiley Online Library on [03/02/2026]. See the Terms and Conditions (https://onlinelibrary.wiley.com/terms-and-conditions) on Wiley Online Library for rules of use; OA articles are governed by the applicable Creative Commons License

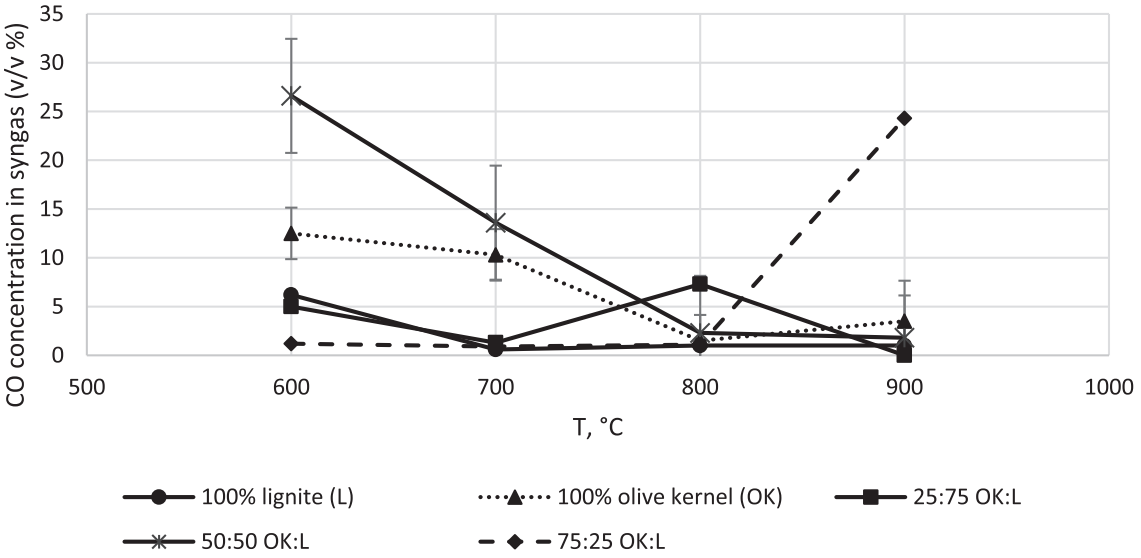


FIGURE 10 | Effect of amount of olive kernel in fuel on carbon monoxide concentration (fuel: w/w%).

TABLE 7 | Hydrogen enhancement factor (EF) values for fuel blends.

T (°C)	EF (25:75 OK:L)	EF (50:50 OK:L)	EF (75:25 OK:L)
600	1.10	1.15	1.36
700	1.00	1.05	1.09
800	0.97	0.99	1.00
900	1.02	1.03	1.00

reforming reaction. Zhuang et al. studied textile gasification under a steam atmosphere and reported that the gasification of volatile matters with steam by the reforming reaction enhances the hydrogen-rich syngas production [66].

3.1 | Synergy Analysis Based on the Hydrogen Enhancement Factor

The synergistic behavior of the fuel blends was evaluated by quantifying the deviation of the experimental hydrogen amount from the theoretically expected values (see Table 7). The expected hydrogen amount for each blend was theoretically calculated using a linear mixing rule based on the hydrogen amounts of the individual fuels at each temperature. This approach assumes that no interaction or modification of reaction pathways occurs during co-gasification and that the mixture behaves as an ideal linear combination of lignite and olive kernel. The expected hydrogen amount is expressed as

$$H_{2,\text{expected}} = x_{\text{Olivekernel}} \cdot H_{2,\text{Olivekernel}} + x_{\text{Lignite}} \cdot H_{2,\text{Lignite}} \quad (8)$$

where $x_{\text{Olive kernel}}$ and x_{Lignite} denote the mass fractions of olive kernel and lignite. The interaction between the fuels was quantified through the enhancement factor EF defined as

$$EF = \frac{H_{2\ \text{experimental}}}{H_{2\ \text{expected}}} \quad (9)$$

Values above unity indicate positive synergy where the blend produces more hydrogen than predicted by the linear rule. Values near unity reflect ideal mixing behavior, whereas values below unity correspond to negative synergy.

The calculated enhancement factors (see Table 7) reveal a clear temperature dependent trend. At 600°C the blends exhibit strong positive synergy and the effect is most pronounced for the 75% olive kernel and 25% lignite mixture where EF = 1.36. This indicates that the hydrogen amount is approximately 35% higher than expected and suggests that the high volatile content and catalytically active ash of olive kernel promote additional hydrogen forming reactions when co-gasified with lignite at lower temperatures. The 50% olive kernel and 50% lignite blend also shows meaningful synergy at 600°C with an enhancement factor of 1.15 which further supports the presence of interactive mechanisms at low temperatures.

At 700°C, mild positive synergy persists for most blends with enhancement factors between 1.05 and 1.09. Although the magnitude of the interaction decreases the mixtures still produce slightly higher hydrogen amounts than expected. Above 800°C the system approaches ideal behavior, and enhancement factors fall within the range of 0.97–1.02 indicating that high temperature gasification is mainly governed by homogeneous reactions rather than blend induced interactions. Overall the synergy analysis confirms that co-feeding olive kernel and lignite enhances hydrogen production primarily at low to intermediate temperatures. The highest synergistic improvement is observed in olive kernel rich mixtures which benefit from accelerated devolatilization and hydrogen generation mechanisms. These results demonstrate that controlled biomass blending can be an effective strategy to improve hydrogen rich syngas production in fluidized bed gasification systems.

3.2 | Implications for Turkish Lignite Resources and Future Research Directions

The practical implications of these findings are particularly relevant within the context of Turkish lignite resources, which

15214125, 2026, 2, Downloaded from https://onlinelibrary.wiley.com/doi/10.1002/ceat.70163 by HAZAL OZTAN - Gazi University , Wiley Online Library on [03/02/2026]. See the Terms and Conditions (https://onlinelibrary.wiley.com/terms-and-conditions) on Wiley Online Library for rules of use; OA articles are governed by the applicable Creative Commons License

exhibit distinct mineralogical and thermochemical characteristics depending on their origin. Lignites from major basins such as Soma and Tunçbilek typically contain elevated volatile matter and moderate alkali content, whereas Çan and Afşin–Elbistan lignites are characterized by very high ash levels, lower calorific values, and abundant Ca–Mg bearing mineral phases that often reduce overall gasification reactivity [67]. The co-gasification of such lignites with potassium-rich biomass residues like olive kernel offers a promising pathway for improving hydrogen-rich syngas formation, as demonstrated by the positive correlation between K/Al ratios and H_2 production. This catalytic enhancement is especially valuable for low-grade lignites such as those from Afşin–Elbistan, where high ash load and limited inherent catalytic minerals constrain char conversion and secondary reforming reactions. Economically, integrating agro-industrial waste materials into lignite-based gasification systems aligns with Türkiye's ongoing efforts to reduce dependence on higher quality imported coals and to utilize regional biomass residues effectively, particularly in the Aegean and Marmara regions where olive kernel is abundantly available [68]. Future work should involve advanced kinetic modeling tailored to site-specific lignite compositions (e.g., Ca-rich Afşin–Elbistan vs. Si–Al dominated Soma lignites), as well as detailed ash fusion and agglomeration analyses to ensure stable operation in fluidized-bed or entrained-flow gasifiers. These steps will support the development of optimized co-gasification frameworks that leverage both local lignite characteristics and regionally available biomass resources.

4 | Conclusion

This study shows that Tunçbilek lignite and olive kernel co-gasification synergy is a quite efficient way to produce hydrogen-rich syngas. Although temperature enhanced the hydrogen concentration in syngas, K/Al and K/Si ratios of olive kernel are quite important co-gasification synergy. Effect of potassium as a natural catalyst in the fuel mixture is essential for syngas composition. In co-gasification studies, the highest hydrogen concentration value was obtained when 25% olive kernel was added to Tunçbilek lignite. It is recommended by this study to incorporate olive kernel as a valuable carbon source in gasification processes at ratios of 25%, 50%, and 75% into Tunçbilek lignite feed (considering the low operating temperature). Consequently, gasification highly promotes both using Tunçbilek lignite and olive kernel as fuel to produce syngas, energy conversion, and conservation in high demand of the country.

Author Contributions

Hazal Öztan: conceptualization, methodology, formal analysis and investigation, writing – original draft preparation. **Duygu Uysal**: conceptualization, methodology, formal analysis and investigation, writing – review and editing. **Özkan Murat Doğan**: conceptualization, funding acquisition, resources, supervision. **Bekir Zühtü Uysal**: conceptualization, funding acquisition, resources, supervision.

Acknowledgments

The authors would like to thank Turkish Coal Enterprise and Bekir TEKERCİOĞLU for providing Tunçbilek lignite. The metal contents of Tunçbilek lignite and olive kernel were analyzed by Meta Nickel Cobalt Mining Industry and Trade Plc. in Research and Development Laboratory Gördes/MANİSA. Thus, the authors would like to thank to Hilal Seda DEMİREL for the contribution in communication with Meta Nickel Cobalt Mining Industry and Trade Plc.

Funding

This study was supported by Gazi University Research Funding [Project No: 06/2007-26].

Conflicts of Interest

The authors declare no conflicts of interest.

Data Availability Statement

Research data are not shared.

References

1. BP, *BP Statistical Review* (BP, 2016), http://large.stanford.edu/courses/2016/ph240/stanchi2/docs/bp-2016.pdf.

2. IEA, *Net Zero Emissions by 2050 Scenario (NZE)* (IEA, 2023), https://www.iea.org/reports/global-energy-and-climate-model/net-zero-emissions-by-2050-scenario-nze.

3. İ. Koçyiğit Çapoğlu, D. Uysal, and Ö. M. Doğan, "Mass Transfer Studies for CO_2 Absorption Into Carbitol Acetate as an Effective Physical Absorbent Using a Laboratory-Scale Packed Column," *Heat and Mass Transfer* 60, no. 1 (2024): 133–145, https://doi.org/10.1007/s00231-023-03427-y.

4. IEA, *World Energy Outlook* (IEA, 2023), https://www.iea.org/reports/world-energy-outlook-2023/executive-summary.

5. H. Schobert, *Chemistry of Fossil Fuels and Biofuels*, 1st ed. (Cambridge University Press, 2013).

6. TKİ, *TKİ Kömür Sektör Raporu (Turkish Coal Enterprises-Coal Sector Report)* (TKİ, 2010).

7. Y. Xia, R. Zhang, Y. Cao, Y. Xing, and X. Gui, "Role of Molecular Simulation in Understanding the Mechanism of Low-Rank Coal Flotation: A Review," *Fuel* 262 (2020): 116535, https://doi.org/10.1016/j.fuel.2019.116535.

8. TKİ. *DÜNYA ve TÜRKİYE KÖMÜR KAYNAK ve REZERV DURUMU (World and Türkiye Coal Resources and Reserve Status)* (TKİ, 2023).

9. O. Kural, *Kömür özellikleri, Teknolojisi Ve Çevre Ilişkileri*, 1st ed. (Özgün Ofset Matbaacılık, 1998).

10. V. Önen and M. K. Karaoğlan, "Flotation of Low-Rank Coal Slimes," *Niğde Ömer Halisdemir Üniversitesi Mühendislik Bilimleri Dergisi* 13, no. 1 (2024): 149–155, https://doi.org/10.28948/ngumuh.1324175.

11. S. Ş. Akın, A. Akgül, and F. Kazanç, "Sodium Salt Surface Interactions Affect Single Particle Combustion Behavior of Biomass, Coal, and Their Chars," *Fuel* 354 (2023): 129259, https://doi.org/10.1016/j.fuel.2023.129259.

12. Ş. Turhan and Y.-D. Jamasali, "Evaluation of Radiological Health Risk Caused by the Use of Fly Ash in Cement and Concrete Production and Its Storage," *International Journal of Environmental Health Research* 34 (2024): 3256–3271, https://doi.org/10.1080/09603123.2023.2301051.

13. B. Gürel, G. K. Dolgun, O. İpek, and A. Keçebaş, "Combustion Characteristics of Low-Quality Lignite for Different Bed Material Sphericities in a Circulating Fluidized Bed Boiler: A Numerical Study," *Particuology* 90 (2024): 364–382, https://doi.org/10.1016/j.partic.2023.12.011.

14. U. Kahraman and I. Dincer, "Development and Assessment of an Integrated Underground Gasification System for Cleaner Outputs," *Energy* 285 (2023): 128676, https://doi.org/10.1016/j.energy.2023.128676.

15214125, 2026, 2, Downloaded from https://onlinelibrary.wiley.com/doi/10.1002/ceat.70163 by HAZAL OZTAN - Gazi University , Wiley Online Library on [03/02/2026]. See the Terms and Conditions (https://onlinelibrary.wiley.com/terms-and-conditions) on Wiley Online Library for rules of use; OA articles are governed by the applicable Creative Commons License

15. M. Varol, "Combustion and Co-Combustion of Olive Cake and Coal in a Fludized Bed Master of Science, Middle East Technical University (Ankara)," (2006).

16. S. Akın, "Biyokütle olarak pirinanın enerji üretiminde kullanılması (in Turkish) Balıkesir University (Faculty of Science and Letters)" (2005).

17. A. Ceylan and B. Kendirli, "Zeytinyağı sektörü atıklarının sera ısıtmasında kullanımı (in Turkish) Süleyman Demirel Üniversitesi Ziraat Fakültesi Dergisi" (2018), 53–61.

18. T. Zhou, W. Zhang, Y. Shen, S. Luo, and D. Ren, "Progress in the Change of Ash Melting Behavior and Slagging Characteristics of Co-Gasification of Biomass and Coal: A Review," *Journal of the Energy Institute* 111 (2023): 101414, https://doi.org/10.1016/j.joei.2023.101414.

19. Ö. Yörük, M. G. Yıldız, D. Uysal, Ö. M. Doğan, and B. Z. Uysal, "Experimental Investigation for Novel Electrode Materials of Coal-Assisted Electrochemical In-Situ Hydrogen Generation: Parametric Studies Using Single-Chamber Cell," *International Journal of Hydrogen Energy* 48, no. 11 (2023): 4173–4181, https://doi.org/10.1016/j.ijhydene.2022.10.275.

20. Y. Yağızatlı, A. Sahin, and İ. Ar, "Synthesized and Characterized High-Performance and Low-Cost Zirconium Phosphate-Additive Sulfonated Polyethersulfone Membranes for PEMFC," *Polymers for Advanced Technologies* 35, no. 6 (2024): e6468, https://doi.org/10.1002/pat.6468.

21. NETL, *Syngas Conversion to Methanol* (NETL, 2024), https://www.netl.doe.gov/research/coal/energy-systems/gasification/gasifipedia/methanol.

22. S. Khan, K. Elkadi, and I. Janajreh, "Investigation of the Co-Gasification Behavior of Kentucky Coal and Palm Woody Biomass," *Procedia Computer Science* 224 (2023): 314–321, https://doi.org/10.1016/j.procs.2023.09.042.

23. R. Li, Z. Yang, and Y. Duan, "Energy, Economic and Environmental Performance Evaluation of Co-Gasification of Coal and Biomass Negative-Carbon Emission System," *Applied Thermal Engineering* 231 (2023): 120917, https://doi.org/10.1016/j.applthermaleng.2023.120917.

24. A. Anniwaer, N. Chaihad, A. Choirun Az Zahra, et al., "Utilization of Fruit Waste for H_2-Rich Syngas Production via Steam Co-Gasification With Brown Coal," *Carbon Resources Conversion* 6, no. 4 (2023): 315–325, https://doi.org/10.1016/j.crcon.2023.04.002.

25. M. Faizan and H. Song, "Critical Review on Catalytic Biomass Gasification: State-of-Art Progress, Technical Challenges, and Perspectives in Future Development," *Journal of Cleaner Production* 408 (2023): 137224, https://doi.org/10.1016/j.jclepro.2023.137224.

26. D. C. de Oliveira, E. E. S. Lora, O. J. Venturini, D. M. Y. Maya, and M. Garcia-Pérez, "Gas Cleaning Systems for Integrating Biomass Gasification With Fischer-Tropsch Synthesis—A Review of Impurity Removal Processes and Their Sequences," *Renewable & Sustainable Energy Reviews* 172 (2023): 113047, https://doi.org/10.1016/j.rser.2022.113047.

27. X. Fu, W. P. Chan, V. Chin, et al., "Converting Sludge to slag Through a High Temperature Slagging Co-Gasification Process: An Evaluation Based on a Demonstration Trial and Life Cycle Assessment," *Chemical Engineering Journal* 468 (2023): 143475, https://doi.org/10.1016/j.cej.2023.143475.

28. J. Wei, M. Wang, B. Li, et al., "Synergy Mechanism of Biochar and Petcoke Co-Combustion Based on Potassium Migration and Transformation," *Fuel Processing Technology* 250 (2023): 107927, https://doi.org/10.1016/j.fuproc.2023.107927.

29. F. Guo, L. Chen, Y. Li, et al., "Review on the Attribute Cognition and Carbon-Ash-Water Separation of Coal Gasification Fine Slag," *Separation and Purification Technology* 320 (2023): 124121, https://doi.org/10.1016/j.seppur.2023.124121.

30. A. Abdalazeez, T. Li, W. Wang, and S. Abuelgasim, "A Brief Review of CO_2 Utilization for Alkali Carbonate Gasification and Biomass/Coal Co-Gasification: Reactivity, Products and Process," *Journal of CO2 Utilization* 43 (2021): 101370, https://doi.org/10.1016/j.jcou.2020.101370.

31. M. Reinmöller, M. Klinger, M. Schreiner, and H. Gutte, "Relationship Between Ash Fusion Temperatures of Ashes From Hard Coal, Brown Coal, and Biomass and Mineral Phases Under Different Atmospheres: A Combined FactSage™ Computational and Network Theoretical Approach," *Fuel* 151 (2015): 118–123, https://doi.org/10.1016/j.fuel.2015.01.036.

32. H. Öztan, İ. K. Çapoğlu, D. Uysal, and Ö. M. Doğan, "A Parametric Study to Optimize the Temperature of Hazelnut and Walnut Shell Gasification for Hydrogen and Methane Production," *Bioresource Technology Reports* 23 (2023): 101581, https://doi.org/10.1016/j.biteb.2023.101581.

33. H. Öztan, D. Uysal, Ö. M. Doğan, and B. Uysal, "Production of H_2-Rich Syngas in a Fluidized Bed," in *10th International 100% Renewable Energy Conference (IRENEC2020)* (2020).

34. J. Kryca, J. Priščák, J. Łojewska, M. Kuba, and H. Hofbauer, "Apparent Kinetics of the Water-Gas-Shift Reaction in Biomass Gasification Using Ash-Layered Olivine as Catalyst," *Chemical Engineering Journal* 346 (2018): 113–119, https://doi.org/10.1016/j.cej.2018.04.032.

35. B. Li, L. Wei, Y. Haiping, X. Wang, and H. Chen, "The Enhancing Mechanism of Calcium Oxide on Water Gas Shift Reaction for Hydrogen Production," *Energy* 68 (2014): 248–254, https://doi.org/10.1016/j.energy.2014.02.088.

36. Y. Zhang, X. Gong, B. Zhang, W. Liu, and M. Xu, "Potassium Catalytic Hydrogen Production in Sorption Enhanced Gasification of Biomass With Steam," *International Journal of Hydrogen Energy* 39 (2014): 4234–4243, https://doi.org/10.1016/j.ijhydene.2014.01.015.

37. P. Basu, *Combustion and Gasification in Fluidized Bed*, 1st ed. (Taylor and Francis Group, 2006).

38. L. Emami-Taba, M. F. Irfan, W. M. A. Wan Daud, and M. H. Chakrabarti, "Fuel Blending Effects on the Co-Gasification of Coal and Biomass—A Review," *Biomass and Bioenergy* 57 (2013): 249–263, https://doi.org/10.1016/j.biombioe.2013.02.043.

39. C. Gao, F. Vejahati, H. Katalambula, and R. Gupta, "Co-Gasification of Biomass With Coal and Oil Sand Coke in a Drop Tube Furnace," *Energy & Fuels* 24, no. 1 (2010): 232–240, https://doi.org/10.1021/ef900578t.

40. M. Mastellone, L. Zaccariello, and U. Arena, "Co-Gasification of Coal, Plastic Waste and Wood in a Bubbling Fluidized Bed Reactor," *Fuel* 89 (2010): 2991–3000, https://doi.org/10.1016/j.fuel.2010.05.019.

41. A. Ramos, E. Monteiro, V. Silva, and A. Rouboa, "Co-Gasification and Recent Developments on Waste-to-Energy Conversion: A Review," *Renewable & Sustainable Energy Reviews* 81 (2018): 380–398, https://doi.org/10.1016/j.rser.2017.07.025.

42. A. A. Ahmad, N. A. Zawawi, F. H. Kasim, A. Inayat, and A. Khasri, "Assessing the Gasification Performance of Biomass: A Review on Biomass Gasification Process Conditions, Optimization and Economic Evaluation," *Renewable & Sustainable Energy Reviews* 53 (2016): 1333–1347, https://doi.org/10.1016/j.rser.2015.09.030.

43. J. F. Vélez, F. Chejne, C. F. Valdés, E. J. Emery, and C. A. Londoño, "Co-Gasification of Colombian Coal and Biomass in Fluidized Bed: An Experimental Study," *Fuel* 88, no. 3 (2009): 424–430, https://doi.org/10.1016/j.fuel.2008.10.018.

44. A. Almeida, P. Neto, I. Pereira, A. Ribeiro, and R. Pilão, "Effect of Temperature on the Gasification of Olive Bagasse Particles," *Journal of the Energy Institute* 92, no. 1 (2019): 153–160, https://doi.org/10.1016/j.joei.2017.10.012.

45. H. Hofbauer and R. Rauch, *Hydrogen Rich Gas From Biomass Steam Gasification* (Sevilla, 2000).

46. G. Blázquez, M. Calero, Á. Gálvez-Pérez, M. Á. Martín-Lara, and A. Pérez, "Bench-Scale Gasification of Olive Cake in a Bubbling Fluidized Bed Reactor," *Applied Sciences* 14, no. 16 (2024): 7282.

47. A. Gálvez-Pérez, M. A. Martín-Lara, M. Calero, A. Pérez, P. Canu, and G. Blázquez, "Experimental Investigation on the Air Gasification of Olive Cake at Low Temperatures," *Fuel Processing Technology* 213 (2021): 106703, https://doi.org/10.1016/j.fuproc.2020.106703.

15214125, 2026, 2, Downloaded from https://onlinelibrary.wiley.com/doi/10.1002/ceat.70163 by HAZAL OZTAN - Gazi University , Wiley Online Library on [03/02/2026]. See the Terms and Conditions (https://onlinelibrary.wiley.com/terms-and-conditions) on Wiley Online Library for rules of use; OA articles are governed by the applicable Creative Commons License

48. G. Matta, D. Semaan, and R. Harb, "Simulation of Olive Pomace Gasification for Hydrogen Production Using Aspen Plus: Case Study Lebanon," *Energies* 17, no. 7 (2024): 1621.

49. B. Hosseingholilou, N. Tavakoli, and M. Saidi, "Cost-Effectiveness and Economic Growth Potential Evaluation of Olive Pomace Gasification Process to Sustainable Fuel: Comparison Study of Different Gasifying Agent," *Process Safety and Environmental Protection* 187 (2024): 533–548, https://doi.org/10.1016/j.psep.2024.04.086.

50. D. Mallick, P. Mahanta, and V. S. Moholkar, "Co-Gasification of Coal and Biomass Blends: Chemistry and Engineering," *Fuel* 204 (2017): 106–128, https://doi.org/10.1016/j.fuel.2017.05.006.

51. J. Xie, W. Zhong, B. Jin, Y. Shao, and H. Liu, "Simulation on Gasification of Forestry Residues in Fluidized Beds by Eulerian–Lagrangian Approach," *Bioresource Technology* 121 (2012): 36–46, https://doi.org/10.1016/j.biortech.2012.06.080.

52. D. S. Upadhyay, K. Panchal, A. K. Sakhiya, and R. N. Patel, "Air-Steam Gasification of Lignite in a Fixed Bed Gasifier: Influence of Steam to Lignite Ratio on Performance of Downdraft Gasifier," *Energy* 211 (2020): 118187, https://doi.org/10.1016/j.energy.2020.118187.

53. M. Khzouz and E. I. Gkanas, "Experimental and Numerical Study of Low Temperature Methane Steam Reforming for Hydrogen Production," *Catalysts* 8, no. 1 (2017): 5, https://doi.org/10.3390/catal8010005.

54. F. Pinto, R. N. André, C. Franco, H. Lopes, I. Gulyurtlu, and I. Cabrita, "Co-Gasification of Coal and Wastes in a Pilot-Scale Installation 1: Effect of Catalysts in Syngas Treatment to Achieve Tar Abatement," *Fuel* 88, no. 12 (2009): 2392–2402, https://doi.org/10.1016/j.fuel.2008.12.012.

55. R. Andre, F. Pinto, C. Franco, et al., "Fluidised Bed Co-Gasification of Coal and Olive Oil Industry Wastes," *Fuel* 84 (2005): 1635–1644, https://doi.org/10.1016/j.fuel.2005.02.018.

56. X. Liu, Y. Tu, X. Xu, and Z.-N. Liu, "The Development and Research Prospect on Catalytic Coal Gasification," *Chemical Engineering Transactions* 61 (2017): 1165–1170, https://doi.org/10.3303/CET1761192.

57. M. S. Masnadi-Shirazi, *Biomass/Fossil Fuel Co-Gasification With and Without Integrated CO_2 Capture* (University of British Columbia, 2014).

58. M. S. Masnadi, J. R. Grace, X. T. Bi, C. J. Lim, and N. Ellis, "From Fossil Fuels Towards Renewables: Inhibitory and Catalytic Effects on Carbon Thermochemical Conversion During Co-Gasification of Biomass With Fossil Fuels," *Applied Energy* 140 (2015): 196–209, https://doi.org/10.1016/j.apenergy.2014.12.006.

59. R. Habibi, J. Kopyscinski, M. S. Masnadi, et al., "Co-Gasification of Biomass and Non-Biomass Feedstocks: Synergistic and Inhibition Effects of Switchgrass Mixed With Sub-Bituminous Coal and Fluid Coke During CO_2 Gasification," *Energy & Fuels* 27, no. 1 (2012): 494–500, https://doi.org/10.1021/ef301567h.

60. V. Nemanova, A. Abedini, T. Liliedahl, and K. Engvall, "Co-Gasification of Petroleum Coke and Biomass," *Fuel* 117 (2014): 870–875, https://doi.org/10.1016/j.fuel.2013.09.050.

61. V. Skoulou, G. Koufodimos, Z. Samaras, and A. Zabaniotou, "Low Temperature Gasification of Olive Kernels in a 5-kW Fluidized Bed Reactor for H_2-Rich Producer Gas," *International Journal of Hydrogen Energy* 33, no. 22 (2008): 6515–6524, https://doi.org/10.1016/j.ijhydene.2008.07.074.

62. D. Feng, Y. Zhao, Y. Zhang, H. Xu, L. Zhang, and S. Sun, "Catalytic Mechanism of Ion-Exchanging Alkali and Alkaline Earth Metallic Species on Biochar Reactivity During CO_2/H_2O Gasification," *Fuel* 212 (2018): 523–532, https://doi.org/10.1016/j.fuel.2017.10.045.

63. Y. Bai, S. Zhu, K. Luo, M. Gao, L. Yan, and F. Li, "Coal Char Gasification in H_2O/CO_2: Release of Alkali and Alkaline Earth Metallic Species and Their Effects on Reactivity," *Applied Thermal Engineering* 112 (2017): 156–163, https://doi.org/10.1016/j.applthermaleng.2016.10.044.

64. L. Ding, Z. Dai, J. Wei, Z. Zhou, and G. Yu, "Catalytic Effects of Alkali Carbonates on Coal Char Gasification," *Journal of the Energy Institute* 90, no. 4 (2017): 588–601, https://doi.org/10.1016/j.joei.2016.05.003.

65. B. Zhao, L. Liu, Q. Liu, N. Li, H. Zhou, and Y. Ban, "Novel Insight Into Calcium-Catalyzed Steam Gasification Behaviors of Lignite," *Fuel* 377 (2024): 132773, https://doi.org/10.1016/j.fuel.2024.132773.

66. X. Zhuang, N. Zhu, F. Li, et al., "Hydrogen-Rich Syngas Production From Waste Textile Gasification Coupling With Catalytic Reforming Under Steam Atmosphere," *Processes* 12, no. 9 (2024): 1790, https://doi.org/10.3390/pr12091790.

67. Ö. Yörük, D. Uysal, and Ö. M. Doğan, "Carbon-Assisted Hydrogen Production via Electrolysis at Intermediate Temperatures: Impact of Mineral Composition, Functional Groups, and Membrane Effects on Current Density," *Fuel* 380 (2025): 133268, https://doi.org/10.1016/j.fuel.2024.133268.

68. H. Öztan and D. Uysal, "Sensitivity Analysis of Steam/Fuel Ratio and Gasification Temperature on Syngas Composition via Thermodynamic Equilibrium Model," *Chemical Engineering Research and Design* 220 (2025): 392–411, https://doi.org/10.1016/j.cherd.2025.06.045.

15214125, 2026, 2, Downloaded from https://onlinelibrary.wiley.com/doi/10.1002/ceat.70163 by HAZAL OZTAN - Gazi University , Wiley Online Library on [03/02/2026]. See the Terms and Conditions (https://onlinelibrary.wiley.com/terms-and-conditions) on Wiley Online Library for rules of use; OA articles are governed by the applicable Creative Commons License